Femtosecond Pump-Probe Spectroscopy of Bacteriochlorophyll *a* Monomers in Solution

Sergei Savikhin and Walter S. Struve
Ames Laboratory, U. S. Department of Energy, and Department of Chemistry Iowa State University, Ames, Iowa 50011 USA

ABSTRACT One- and two-color absorption difference profiles were obtained for BChl *a* in 1-propanol with ~50-fs resolution, using a self-mode-locked Ti:sapphire laser system. Time evolution in the BChl *a* absorption difference spectrum produces nonexponential photobleaching/stimulated emission (PB/SE) decay kinetics in 800-nm one-color experiments. Nonexponential PB/SE rise behavior occurs for some combinations of pump and probe wavelengths in two-color experiments. Optimized parameters from triexponential fits to the absorption difference profiles depend markedly on the fitting time window; they typically include a minor component with lifetime in the hundreds of fs. Much of the latter component is due to vibrational relaxation and/or intramolecular vibrational redistribution, rather than solvent dielectric relaxation. Measurements of the pump-probe anisotropy indicate that the electronic transition moment for the broad Q_y excited state absorption band that overlaps the Q_y steady-state absorption spectrum makes an angle of at most 20° from that of the ground → Q_y state transition. No coherent oscillations are observed at early times. Our results bear directly on the interpretation of fs pump-probe experiments on BChl *a* - containing pigment-protein complexes.

INTRODUCTION

The recent emergence of self-mode-locked Ti:sapphire lasers in ultrafast photosynthesis laboratories has greatly facilitated the study of sub-ps energy transfer kinetics in pigment-protein complexes from green and purple photosynthetic bacteria (Savikhin et al., 1994; Chachisvilis et al., 1994). For example, spectral equilibration has now been observed with 300–450 fs kinetics among inequivalent bacteriochlorophyll (BChl) *a* antenna pigments in pump-probe experiments (Savikhin et al., 1994) on Fenna-Matthews-Olson (FMO) trimers from the green thermophilic bacterium *Chlorobium tepidum* (Tronrud et al., 1986; Blankenship et al., 1993). Similarly, the pump-probe anisotropy decay kinetics in this well-known BChl *a* protein are now known to be nonexponential, with major lifetime components of 75–100 fs and 1.7–2.2 ps (Savikhin et al., 1994; S. Savikhin and W. S. Struve, unpublished work). The latter component, which is not mirrored in any major isotropic decay component for FMO trimers, probably corresponds to equilibration of excitation among the lowest-energy, rotationally equivalent pigments in this antenna.

A complication in the interpretation of pump-probe experiments in BChl *a*-containing antennae is the possibility of ultrafast processes unrelated to energy transfer and trapping, such as vibrational cooling, intramolecular vibrational redistribution (IVR), and dielectric relaxation. Becker et al. (1991) investigated the transient absorption behavior of BChl *a* monomers in several polar solvents by exciting them in the Q_x band with laser pulses 0.8 ps wide. The photobleaching/stimulated emission (PB/SE) peak in the broadband absorption difference spectrum was observed to shift to the red by ~5–9 nm with solvent-dependent kinetics. Biexponential fits to the Stokes shift kinetics in the PB/SE band maximum yielded the lifetimes 1.5, 18 ps in methanol, and 1.1, 82 ps in 1-propanol. The spectral shifting was well described by single-exponential model with 2.7 ps lifetime in pyridine. Such solvent dependence suggested that IVR is not a major contributor to the ps spectral evolution; the observed red shifts may stem from vibrational cooling and/or dielectric relaxation. In this paper, we have extended the work of Becker et al. (1991) by exciting BChl *a* monomers directly in the Q_y band with 760–800 nm pulses ≤100 fs wide. We can thus compare the kinetics of BChl *a* monomers in solution with those observed in BChl *a*-containing pigment-protein complexes under similar experimental conditions to ascertain the extent to which single-pigment processes may contribute to the fs kinetics in the latter systems. A second issue of interest to us is the polarization of the broad Q_y excited state absorption (ESA) band, which overlaps the Q_y state photobleaching and stimulated emission bands in BChl *a* (Becker et al., 1991). Interpretations of pump-probe depolarization studies in pigment-protein complexes have tacitly assumed either that the ESA cross section at the probe wavelength in Chl or BChl pigments is small compared with those of PB and SE, or that its polarization is essentially parallel to those of PB and SE (Lin et al., 1991; Kwa et al., 1992; Savikhin et al., 1994). The ESA cross section for BChl *a* in methanol at 770 nm (the position of its Q_y band maximum in that solvent) is in fact ~1/2 of the ground-state absorption cross section (Becker et al., 1991), so that ESA potentially exerts a major effect on the pump-probe anisotropy if its transition moment is not parallel to that of PB/SE. We report here the observation of fs absorption difference components for BChl *a* in 1-propanol. For given probe wavelength, the qualitative absorption difference profiles are sensitive to the excitation wavelength, and the spectral shifts

Received for publication 1 June 1994 and in final form 28 August 1994.
Address reprint requests to Dr. Walter S. Struve, Department of Chemistry, Iowa State University, Gilman Hall, Ames, IA 50011-3111. Tel.: 515-294-4276; Fax: 515-294-1699; E-mail: wstruve @ameslab.gov.

0006-3495/94/11/2002/06 $2.00

appear to contain substantial contributions from vibrational cooling and/or IVR. Finally, our anisotropy studies of BChl *a* in 1-propanol indicate that its ESA transition moment at 760 and 777 nm is nearly parallel to the ground state → Q_y transition moment.

MATERIALS AND METHODS

The self-mode-locked Ti:sapphire laser system, group velocity dispersion (GVD) compensation optics, and radio-frequency multiple modulation detection system have been described previously (Anfinrud and Struve, 1986; Savikhin et al., 1994). In one-color experiments, laser tuning was achieved with a single-plate birefringent filter, yielding ~80 fs pulses with 8–10 nm spectral bandwidth and ~120 fs autocorrelation function. Typical Ti:sapphire output power for 5 W multiline Ar^+ pump power was 600 mW at 740 nm. In two-color experiments, the birefringent filter was omitted, and the output pulses were ~40 fs wide with 20–40 nm bandwidth. The pump and probe pulse spectra were shaped using interference bandpass filters (CVI Laser Corporation, Albuquerque, NM) centered at the selected wavelengths. The resulting spectral narrowing (~7 nm) increased the laser cross-correlation function to 160–220 fs, depending on the interference filters used. The apparatus instrument function used for convolute-and-compare analyses of the absorption difference profiles was recorded simultaneously with every pump-probe scan, using a portion of the pump and probe beams focused into an $LiIO_3$ nonlinear crystal. Samples of BChl *a* (obtained from Sigma Chemical Co. (St. Louis, MO) as isolated from *Rhodopseudomonas sphaeroides*) were prepared in spectroscopic grade 1-propanol in an N_2 atmosphere, and were housed in a 7.6 cm diameter centrifugal cell capable of rotation at speeds up to 3000 rpm (Savikhin et al., 1993b). An absorption spectrum of BChl *a* in 1-propanol is shown in Fig. 1. This spectrum is essentially invariant over the concentration range 10^{-3}-1 mM, indicating that BChl *a* aggregates are not prevalent in these solutions. BChl *a* optical densities at 777 nm were typically 0.4 in the 0.5-mm path length of the centrifugal sample cell. At this concentration, the most probable nearest-neighbor separation is ~125 Å ($R_{mp} = (2\pi\rho)^{-1/3}$ if the pigments are randomly distributed; ρ is the pigment number density). Hence, negligible electronic energy transfer occurs during the time windows used in this work. A typical isotropic absorption difference profile reported in this work was compiled from an average over 10 individual pump-probe scans; the observed absorption difference kinetics did not change with laser exposure.

RESULTS

The 800-nm isotropic pump-probe kinetics are shown in Fig. 2 for BChl *a* in 1-propanol. This one-color signal is dominated by a large coherent coupling artifact (Vardeny and Tauc, 1981) at times <200 fs. Triexponential fits to 800-nm one-color profiles at later times yield the PB/SE decay components 440 fs (23%), 15 ps (30%), and >1000 ps (47%) when the fitting time window is 8 ps; and 1.7 ps (18%), 17 ps (18%), and >1000 ps (64%) when the time window is 24 ps. In Fig. 3, we show two-color absorption difference signals for the same system. These two-color profiles show no coherent spike, because the 7-nm bandwidth pump and probe pulses have no spectral overlap. Unlike the 800-nm one-color profiles, the 770 → 800-nm two-color profiles (excited and probed at 770 and 800 nm, respectively) exhibit resolvable PB/SE rise kinetics. Triexponential fits to these profiles yield (apart from a decay component with lifetime >1000 ps) PB/SE rise components with lifetimes 270 fs (18%) and 3.8 ps (17%) in an 8-ps time window, and rise components with lifetimes 840 fs (11%) and 16 ps (20%) in an 80-ps time window. Substantial prompt (pulse-limited) rise components

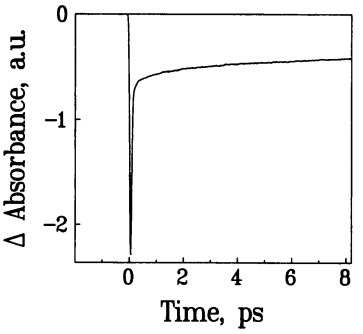

FIGURE 2 One-color isotropic absorption difference profile at 800 nm for BChl *a* in 1-propanol in 8-ps time window, obtained using probe pulses polarized at the magic angle (54.7°) from pump polarization. Negative signal corresponds to PB/SE.

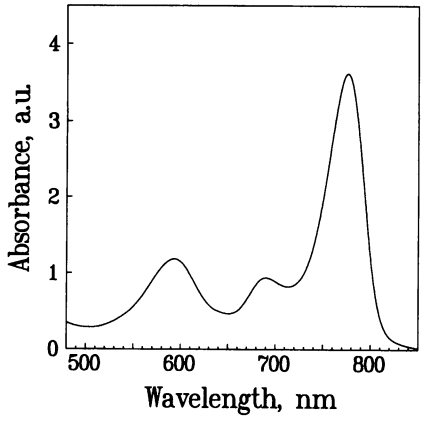

FIGURE 1 Absorption spectrum of BChl *a* monomers in 1-propanol.

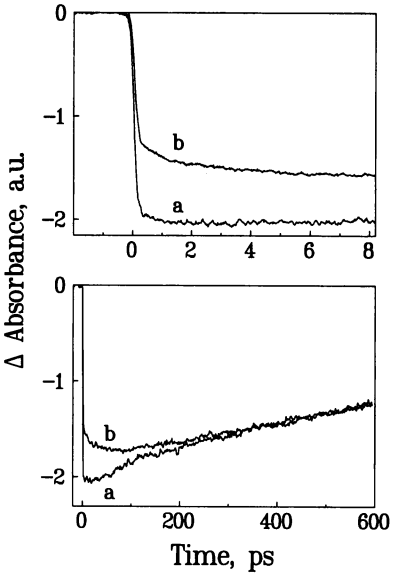

FIGURE 3 Two-color absorption difference profiles for BChl *a* in 1-propanol in 8-ps time window (above) and 590-ps time window (below). Curves a and b give 790 → 820- and 770 → 800-nm profiles, respectively.

are also present (65–70% amplitude in both windows). Since the optimized lifetimes are sensitive to the fitting window, the true rise kinetics in the 770 → 800-nm experiment are clearly not well described during the first 80 ps by a single triexponential model. Becker et al. (1991) showed that the Q_y ESA spectrum of BChl *a* monomers is spectrally broad, with a maximum cross section ~½ those of the Q_y PB and SE bands. The total BChl *a* absorption difference spectrum exhibits a deep trough, with its minimum located between the PB and SE band maxima. The steady-state absorption and emission maxima of BChl *a* in 1-propanol occur at ~776 and 795 nm respectively; the ultrafast PB/SE decay components in our 800-nm one-color experiments (and the rise components in the 770 → 800 nm two-color experiment) arise principally from dynamic spectral shifting in the BChl *a* monomer PB/SE spectrum.

Fig. 3 also offers a comparison between different two-color profiles (770 → 800 and 790 → 820 nm) in which the sample is probed 30 nm downhill from the excitation wavelength. These excitation wavelengths are near the Q_y absorption band maximum and on the red edge of the Q_y band in 1-propanol, respectively. The 770 → 800-nm profiles exhibit considerably more prominent PB/SE rise kinetics than the 790 → 820-nm profiles. In Fig. 4, we show two-color profiles excited at 760, 770, 780, and 800 nm; the probe wavelength is 20 nm downhill from the pump wavelength in each case. None of the latter profiles show a large (>5%) PB/SE rise component, unlike the profiles probed 30 nm downhill from the pump wavelength (Fig. 3). An interesting feature here is presence in the 800 → 820-nm profile of a large ultrafast PB/SE decay component, which is largely absent in the other three profiles. The 800 → 820-nm profile also differs qualitatively from the 790 → 820-nm profile, which exhibits PB/SE rise instead of decay behavior at early times (Fig. 3). These facts are collectively inconsistent with the hypothesis that dynamic red shifting occurs in the BChl *a* PB/SE spectrum, irrespective of excitation wavelength. They can be rationalized if the spectral evolution is dominated by red shifting under most Q_y excitation wavelengths, and by blue shifting when the extreme red edge of the Q_y band is excited (≥800 nm). In this view, the ultrafast PB/SE decay components observed in the 800 → 820-nm experiment (but not in the other two-color experiments in Figs. 3 or 4) appear because 800-nm laser excitation prepares a Q_y vibrational state that is spectroscopically cooler than the vibrationally thermalized Q_y state. Finally, we point out the dissimilarity between the 770 → 800- and 780 → 800-nm profiles and the dissimilarity between the 800 → 820- and 790 → 820-nm profiles. These comparisons emphasize that the BChl *a* pump-probe kinetics observed at a given probe wavelength depend on the excitation wavelength.

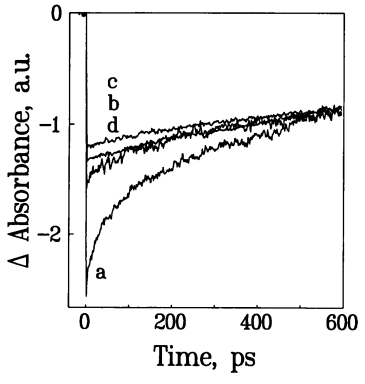

FIGURE 4 Two-color absorption difference profiles for BChl *a* in 1-propanol: a, 800 → 820 nm; b, 780 → 800 nm; c, 770 → 790 nm; and d, 760 → 780 nm.

Optimized fitting parameters for a number of our pump-probe profiles for BChl *a* in 1-propanol are summarized in Table 1.

While the present experiments are capable of detecting vibrational coherences similar to those found in bacterial reaction centers (Vos et al., 1993), we do not observe such oscillations for BChl *a* in 1-propanol at room temperature (cf. Figs. 2–4). Vibrational coherences do appear in the pump-probe spectroscopy of the LH1 BChl *a*-protein antenna from *R. sphaeroides* (Chachisvilis et al., 1994). It remains unclear whether the presence of oscillations in the LH1 antenna and in bacterial reaction centers (as well as their absence in the present work) originates from vibrational modes unique to the pigment-protein complexes, or whether the BChl *a* environments exert large variations in vibrational mode couplings and coherence times. The pigment-protein structure in these complexes may show weaker couplings between BChl *a* modes and the bath, giving rise to slower vibrational dephasing than in solution. Numerous laser dye solutions exhibit similar coherences in their spontaneous fluorescence (Mokhtari et al., 1990) and pump-probe spectroscopy (Wise et al., 1987); many others do not. We have characterized reproducible low-frequency oscillations in one- and two-color profiles for the BChl *c* antenna in chlorosomes from the green bacterium *Chloroflexus aurantiacus*, using the present apparatus (S. Savikhin, Y. Zhu, S. Lin, R. E. Blankenship, and W. S. Struve, unpublished work).

The one-color anisotropy $r(t)$ at 775 nm was obtained by averaging several pairs of profiles $\Delta A_{\parallel}(t)$, $\Delta A_{\perp}(t)$, and then computing $r(t) = [\Delta A_{\parallel}(t) - \Delta A^{\perp}(t)]/[\Delta A_{\parallel}(t) + 2\Delta A_{\perp}(t)]$. The result is shown in Fig. 5. Aside from the region of the coherent spike, there is little if any discernible decay in $r(t)$ during the first 8 ps; rotational diffusion of BChl *a* monomers in 1-propanol is slow on this time scale, as are electronic energy transfers among monomers at the present concentrations. This figure also shows that the upper limit on the initial anisotropy $r(0)$ is approximately 0.41. Anisotropy measurements at 760 nm similarly indicate that $r(0)$ at this wavelength is 0.42 ± 0.03.

DISCUSSION

Our isotropic absorption difference profiles for BChl *a* in 1-propanol are nonexponential. Triexponential fits to these profiles typically yield short components with lifetimes in the hundreds of fs, and the question arises as to whether the

TABLE 1 Optimized parameters for BChl *a* pump-probe profiles in 1-propanol*

$\lambda_{pump} \rightarrow \lambda_{probe}$, nm	Windows, ps	τ_1, ps (A_1)	τ_2, ps (A_2)	τ_3, ps (A_3)	τ_4, ps (A_4)
770 → 800	590			39 (0.18)	1450 (−1.00)
	590		15 (0.13)	137 (0.13)	1250 (−1.00)
	8	0.59 (0.14)	4.2 (0.13)		*1250* (−1.00)
	Global‡	0.77 (0.13)	11 (0.11)	71 (0.13)	1360 (−1.00)
790 → 820	590		23 (0.32)	30 (−0.33)	1270 (−0.67)
	8	0.39 (0.12)			∞ (−1.00)
760 → 780	590			98 (−0.19)	1860 (−0.81)
	8			15 (−0.20)	1760 (−0.80)
770 → 790	590			219 (−0.12)	*2850* (−0.88)
	82			884 (−0.44)	*2850* (−0.56)
	8	0.54 (0.05)		826 (−0.45)	2850 (−0.55)
780 → 800	590			1100 (−0.70)	2850 (−0.30)
	8			985 (−0.66)	3670 (−0.34)
800 → 820	590		3.4 (−0.10)	50 (−0.23)	874 (−0.66)
	82		1.7 (−0.15)	30 (−0.20)	*874* (−0.66)
	24		1.7 (−0.18)	64 (−0.29)	*874* (−0.53)
	8	0.51 (−0.14)		11 (−0.21)	*874* (−0.65)

* Negative amplitudes correspond to PB/SE decay; parameters in italicized figures were held fixed.
‡ Global fit of four profiles measured using 8, 24, 82, and 590-ps windows.

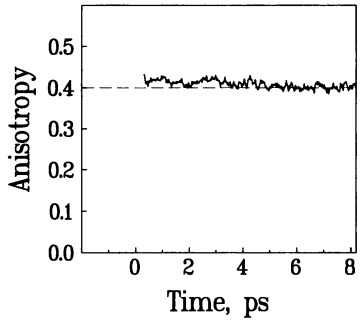

FIGURE 5 One-color anisotropy decay function $r(t)$ at 775 nm for BChl *a* monomers in 1-propanol, computed from the polarized absorption difference signals $\Delta A_{\parallel}(t)$ and $\Delta A_{\perp}(t)$.

origin of these components in solution can also account for the major sub-ps components observed in the pump-probe spectroscopy of BChl *a* pigment-protein complexes (Savikhin et al., 1994). In studying the ps dynamics of BChl *a* in several solvents, Becker et al. (1991) considered vibrational cooling, IVR, and solvent dielectric relaxation as possible mechanisms for their observed red shifts. Since the observed kinetics were sensitive to the solvent, vibrational cooling and dielectric relaxation were considered the most likely origins of the 1.1-ps and 82-ps PB/SE peak shift components for BChl *a* in 1-propanol. In principle, dielectric relaxation could be obviated by studying the kinetics in nonpolar solvents. However, BChl *a* tends to dimerize in very dry nonpolar solvents, using the acetyl group of one molecule as an axial ligand to the second molecule (W. W. Parson, private communication).

We base the discussion of our results on Table 2, which lists the possible combinations of time regimes for vibrational cooling/IVR and dielectric relaxation. In this table, the terms fast, measurable, and slow indicate the kinetics relative to the time windows used in this work. Several improbable cases are included for completeness. In case 1, for example, vibrational equilibration and dielectric relaxation are both

TABLE 2 Dynamic scenarios for vibrational cooling, IVR, and dielectric relaxation of BChl a monomers in solution

Case	Vibrational cooling/ IVR	Dielectric relaxation	Result
1	fast	fast	No spectral evolution; SE solvated and vibrationally thermalized
2	fast	measurable	Kinetics at λ_{probe} independent of λ_{pump}; SE experiences red shift
3	fast	slow	No spectral evolution; SE vibrationally thermalized but unsolvated
4	measurable	fast	Kinetics at λ_{probe} depend on λ_{pump}; SE is solvated; SE experiences red or blue shift
5	measurable	measurable	Kinetics at λ_{probe} depend on λ_{pump}; SE experiences red or blue shift
6	measurable	slow	Kinetics at λ_{probe} depend on λ_{pump}; SE is unsolvated; SE experiences red or blue shift
7	slow	fast	No spectral evolution; SE is Franck-Condon and solvated
8	slow	measurable	Kinetics at λ_{probe} depend on λ_{pump}; SE is Franck-Condon and experiences red shift
9	slow	slow	No spectral evolution; SE is Franck-Condon and unsolvated

essentially complete by 50–100 fs, our time-resolution limit. Since the Q_y ESA spectrum is broad (Becker et al., 1991), the observed spectral evolution is expected to be dominated by changes in the PB/SE spectrum. Cases 1, 3, 7, and 9 can be eliminated a priori, because no spectral evolution would occur in any of these cases where both vibrational equilibration and dielectric relaxation are either slow or fast compared to the time window. Case 2 (measurable dielectric relaxation following fast vibrational thermalization) can be ruled out, because the observed profiles for given probe wavelength depend markedly on the pump wavelength (cf. the observed contrasts among the 770 → 800-, 780 → 800-, and 800 → 800-nm pump-probe profiles). Case 8 (dielectric relaxation of SE that remains Franck-Condon in the intramolecular

modes) can similarly be ruled out, because the 800 → 820 nm profile shows evidence for an SE blue shift when the BChl *a* Q_y spectrum is excited at its extreme red edge. Hence, vibrational equilibration/IVR is a major contributor to the observed fs and ps kinetics of BChl *a* in 1-propanol. Our data alone cannot distinguish among the remaining cases (4–6).

In this context, it appears relevant that a variety of dielectric relaxation time constants have been reported for different probe molecules in 1-propanol and 1-butanol: 17 and 100 ps for the laser dye LDS-750 in 1-butanol (Castner et al., 1987); <30 ps and 60 ps for coumarin 153 in 1-propanol (Maroncelli and Fleming, 1987); and ~100 ps for 7-amino- and 7-dimethylamino-3-methyl-1,4-benzoxazine-2-one in 1-propanol (Declémy et al., 1987). Our lifetimes for BChl *a* in 1-propanol cannot be compared directly to those reported by Becker et al. (1991), because the initial vibrational energy distributions differ in the two cases. The vibrationally hot modes in the Q_y state following Q_x band excitation will be principally the acceptor modes in $Q_x \rightarrow Q_y$ internal conversion (primarily high-frequency C-H modes; Avouris et al., 1978); the Q_y state is created with excess energy on the order of the Q_x–Q_y band gap (3500–4000 cm^{-1}). The initial vibrational energy distributions in our experiments are determined instead by Franck-Condon factors for the ground → Q_y electronic transition. The excess vibrational energies studied here are conservatively <800 cm^{-1}, and pump wavelengths as long as 800 nm excite primarily hot bands. Hence, our experiments study vibrational equilibration rather than just cooling of vibrationally hot states. Rodriguez et al. (1991) studied porphyrins prepared in excited states with 1–2 eV (8000–16000 cm^{-1}) of excess vibrational energy. In this extreme, the observed spectral evolution appears to be dominated by changes in the electronic band gap, vibrationally induced through anharmonic expansion and/or vibronic coupling. In the present work (where the excess vibrational energies are limited to the much smaller ranges encountered when spectrally disperse BChl *a* antennae are excited in their Q_y bands), such electronic-vibrational couplings are unlikely to be significant.

The marked wavelength sensitivity observed in the amplitudes of the fs components in absorption difference profiles for FMO trimers (Savikhin et al., 1994) indicates that they are strongly influenced by electronic energy transfer. The FMO trimer absorption spectrum (which comprises 21 overlapping exciton components at 14 different wavelengths) is so congested that any wavelength between ~780 and 830 nm yields near-resonant excitation of at least one exciton component. The fs kinetics of FMO trimer one-color profiles would thus be nearly independent of wavelength if they were dominated by vibrational thermalization in the absence of energy transfer. However, the relative amplitudes of one-color fs PB/SE decay components for FMO trimers decrease sharply and monotonically as the wavelength is tuned from 780 to 820 nm (Savikhin et al., 1994; Savikhin and Struve, unpublished work). For example, the 773-nm one-color profile for FMO trimers exhibits a prompt PB/SE signal, which is supplanted within 300 fs by an ESA signal. Since the zero-crossing point between the ESA- and PB/SE-dominated regions of the BChl *a* absorption difference spectrum is situated ~50 nm to the blue of the minimum in the PB/SE trough (Becker et al., 1991), the fs switching of signal polarity from PB/SE to ESA cannot arise from vibrational cooling alone (which can cause spectral shifts of at most 15–25 nm, the wavelength separation between the steady-state absorption and stimulated emission peaks in polar solvents). Rather, it must arise from energy transfer between BChl *a* pigments whose peak Q_y wavelengths are separated by ≥40–50 nm. Similarly, two-color profiles in which the probe wavelength is 30 nm downhill from the pump wavelength exhibit fs rise kinetics when the pump wavelength is 800 or 790 nm, but show fs decay kinetics when the pump wavelength is 770 nm (Savikhin and Struve, unpublished work). This behavior is inconsistent with the assignment of the fs components to vibrational cooling and IVR alone, because each of these pump wavelengths near-resonantly excites a different set of pigments in FMO trimers. However, vibrational equilibration may account for a weak fs PB/SE decay component that is observed in the 830-nm one-color experiment, since this wavelength excites the extreme red edge of the FMO Q_y spectrum. This situation would be analogous to the present 800 → 820-nm experiment (Fig. 4), in which BChl *a* monomers are excited at red edge of their Q_y band.

We finally consider the initial anisotropies $r(0)$ expected for different orientations of the Q_y ESA transition moment μ_{ESA}. It is assumed that the transition moments μ_{PB} and μ_{SE} for Q_y PB and SE are parallel, while γ denotes the direction cosine for μ_{ESA} relative to μ_{PB} or μ_{SE}. The orientationally averaged expressions for the polarized absorption difference signals at zero time (Lyle and Struve, 1991).

$$\Delta A_{\parallel}(0) = -\sigma_{PB}(\sigma_{PB} + \sigma_{SE})\langle\mu_{PB,x}^4\rangle + \sigma_{PB}\sigma_{ESA}\langle\mu_{PB,x}^2\mu_{ESA,x}^2\rangle \quad (1)$$

$$\Delta A_{\perp}(0) = -\sigma_{PB}(\sigma_{PB} + \sigma_{SE})\langle\mu_{PB,x}^2\mu_{PB,y}^2\rangle + \sigma_{PB}\sigma_{ESA}\langle\mu_{PB,x}^2\mu_{ESA,y}^2\rangle$$

then lead to the initial anisotropy

$$r(0) = \frac{2(\sigma_{PB} + \sigma_{SE}) + \sigma_{ESA}(1 - 3\gamma^2)}{5(\sigma_{PB} + \sigma_{SE} - \sigma_{ESA})} \quad (2)$$

where σ_{PB}, σ_{SE}, and σ_{ESA} denote the cross sections for PB, SE, and ESA at the pertinent wavelength. For $\gamma = 1$ (i.e., ESA transition moment parallel to PB/SE transition moments), Eq. 2 predicts that $r(0) = 0.4$, irrespective of the three cross sections. When $\gamma = 0$ (ESA transition moment perpendicular to the PB/SE transition moments), $r(0)$ can be either greater than 0.4 or less than −0.2 (Savikhin et al., 1993a), depending on the value of $\sigma_{ESA}/(\sigma_{PB} + \sigma_{SE})$. Examination of the pertinent wavelength-dependent cross sections for BChl *a* in methanol (Becker et al., 1991), along with consideration of the 2–5 nm solvent shifts between the absorption and fluorescence maxima for BChl *a* in methanol and 1-propanol, suggests that the relative cross sections for PB, SE, and ESA

are on the order of σ, $\sigma/3$, and $\sigma/2$ under the conditions of the 775 nm anisotropy experiment in 1-propanol (Fig. 5). The initial anisotropy predicted at 775 nm for $\mu_{SE} \perp \mu_{PB}$ is then $r(0) = 0.76$. Under the conditions of the 760-nm anisotropy measurements in 1-propanol (which yield $r(0) = 0.42 \pm 0.03$), the relative cross sections are approximately σ, $\sigma/10$, and $\sigma/2$; the predicted initial anisotropy at this wavelength is $r(0) = 0.90$. Alternatively, Eq. 2 can be used to calculate the angle between the transition moments μ_{ESA} and μ_{PB}, given the measured anisotropies at 775 and 760 nm. The measured anisotropies at these wavelengths correspond to an angle of ~12° between μ_{ESA} and μ_{PB}. Given the errors in these measurements, this angle could be as large as 20°. The foregoing analysis is based on the assumption that the PB and SE transition moments are parallel. The broad BChl *a* Q_y ESA band may actually be a superimposition of several excited state absorption bands, and different ESA transition moment orientations may be found at other wavelengths. The present experiments have focused on wavelengths near the Q_y absorption band maximum (777 nm) and on shorter wavelengths (760 nm) where ESA gains more importance relative to SE.

The Ames Laboratory is operated for the U. S. Department of Energy by Iowa State University under Contract No. W-7405-Eng-82. This work was supported by the Division of Chemical Sciences, Office of Basic Energy Sciences.

REFERENCES

Anfinrud, P., and W. S. Struve. 1986. Optical shot-noise-limited detection: a single-sideband technique with flexible modulation frequencies. *Rev. Sci. Instrum.* 57:380–383.

Avouris, P., W. M. Gelbart, and M. A. El-Sayed. 1977. Nonradiative electronic relaxation under collision-free conditions. *Chem. Rev.* 77:793–834.

Becker, M., V. Nagarajan, and W. W. Parson. 1991. Properties of the excited-singlet states of bacteriochlorophyll a and bacteriopheophytin a in Polar Solvents. *Biochemistry.* 113:6840–6848.

Blankenship, R. E., P. Cheng, T. P. Causgrove, D. C. Brune, S. H.-H. Wang, J.-U. Choh, and J. Wang. 1993. Redox regulation of energy transfer in antennas of green photosynthetic bacteria. *Photochem. Photobiol.* 57: 103–107.

Castner, E. W., M. Maroncelli, and G. R. Fleming. 1987. Subpicosecond studies of solvation dynamics in polar aprotic and alcohol solvents. *J. Chem. Phys.* 86:1090–1097.

Chachisvilis, M., T. Pullerits, M. R. Jones, C. N. Hunter, and V. Sundström. 1994. Coherent nuclear motions and exciton state dynamics in photosynthetic light-harvesting pigments. *In* Ultrafast Phenomena. P. F. Barbara and W. H. Knox, editors. Springer-Verlag, Berlin, in press.

Declémy, A., C. Rullière, and P. Kottis. 1987. Picosecond solvation of electronically excited solutes in alcoholic solvents: nonDebye behaviour of the time-dependent fluorescence shift related to hydrogen bonding. *Chem. Phys. Letts.* 133:448–454.

Kwa, S. L. S., H. van Amerongen, S. Lin, J. P. Dekker, R. van Grondelle, and W. S. Struve. 1992. Ultrafast energy transfer in LHC-II trimers from the Chl *a/b* light-harvesting antenna of Photosystem II. *Biochim. Biophys. Acta.* 1102:202–212.

Lin S., H. van Amerongen, and W. S. Struve. 1991. Ultrafast pump-probe spectroscopy of bacteriochlorophyll c antennae in bacteriochlorophyll *a*-containing chlorosomes from the green photosynthetic bacterium *Chloroflexus aurantiacus*. *Biochim. Biophys. Acta.* 1060:13–24.

Lyle, P. A., and W. S. Struve. 1991. Dynamic linear dichroism in chromoproteins. *Photochem. Photobiol.* 33:359–365.

Maroncelli, M., and G. R. Fleming. 1987. Picosecond solvation dynamics of coumarin 153: the importance of molecular aspects of solvation. *J. Phys. Chem.* 86:6221–6239.

Mokhtari, A., A. Chebira, and J. Chesnoy. 1990. Subpicosecond fluorescence dynamics of dye molecules. *J. Opt. Soc. Am.* B7:1551–1557.

Rodriguez, J., C. Kirmaier, and D. Holten. 1991. Time-resolved and static optical properties of vibrationally excited porphyrins. *J. Chem. Phys.* 94:6020–6029.

Savikhin, S., N. Tao, P.-S. Song, and W. S. Struve. 1993a. Ultrafast pump-probe spectroscopy of the photoreceptor stentorins from the ciliate *Stentor coeruleus*. *J. Phys. Chem.* 97:12379–12386.

Savikhin, S., T. Wells, P.-S. Song, and W. S. Struve. 1993b. Ultrafast pump-probe spectroscopy of native etiolated oat phytochrome. *Biochemistry.* 32:7512–7518.

Savikhin, S., W. Zhou, R. E. Blankenship, and W. S. Struve. 1994. Femtosecond energy transfer and spectral equilibration in bacteriochlorophyll *a*-protein antenna trimers from the green bacterium *Chlorobium tepidum*. *Biophys. J.* 66:110–114.

Tronrud, D. E., M. F. Schmid, and B. W. Matthews. 1986. Structure and X-ray amino acid sequence of a bacteriochlorophyll *a* protein from *Prosthecochloris* refined at 1.9 Å resolution. *J. Mol. Biol.* 188:443–454.

Vardeny, Z., and J. Tauc. 1981. Picosecond coherence coupling in the pump and probe technique. *Optics Comms.* 39:396–400.

Vos, M. H., F. Rappaport, J.-C. Lambry, J. Breton, and J.-L. Martin. 1993. Visualization of coherent nuclear motion in a membrane protein by femtosecond spectroscopy. *Nature.* 363:320–325.

Wise, F. W., M. J. Rosker, and C. L. Tang. 1987. Oscillatory femtosecond relaxation of photoexcited organic molecules. *J. Chem. Phys.* 86:2827–2832.